文章编号: 1001－2060(2004)06－0589－04

薄液膜二维表面驻波的流动稳定性研究

叶学民, 李春曦, 阎维平
(华北电力大学 动力工程系, 河北　保定 071003)

摘　要: 驻波作为薄液膜表面波中的一种波, 其流动稳定性受界面热不平衡效应的影响。基于边界层理论和界面热不平衡效应, 推导出沿倾斜壁面下降的在蒸发、等温和冷凝状态下普遍适用的二维表面驻波空间稳定性方程, 从理论上深入分析了热不平衡效应、流体物性、壁面倾角和雷诺数对驻波稳定性的影响。研究表明: 热不平衡效应对驻波稳定性的影响仅在小雷诺数下较为明显, 在高雷诺数下, 稳定性主要取决于惯性力和粘性力; 流体物性和壁面倾角在整个雷诺数范围内均起着非常明显的作用。

关　键　词: 蒸发; 冷却; 热不平衡效应; 薄液膜; 驻波; 稳定性
中图分类号: TK124; O357.1　　文献标识码: A

1　引　言

液体薄膜流作为一种高效传热传质技术, 已在传统工业和高新技术领域得到了广泛的应用。下降中的薄液膜受小扰动因素的影响, 将引起流动结构和状态的改变, 导致表面出现波动。如果引发流动不稳定的小扰动趋于减小, 则流动是稳定的; 反之, 则处于不稳定状态; 如果扰动始终不变, 则流动处于中性稳定状态。

对液膜稳定性的理论研究始于 Benjamin 和 Yih 对等温降膜中行波的线性稳定性分析[1~2]。之后, 基于边界层理论, 一些研究者采用不同方法在不同雷诺数范围内对于蒸发、等温或冷凝状态下的薄液膜二维表面行波进行了线性稳定性分析[3~9]。液膜在下降过程中, 表面波中不仅存在行波, 而且存在驻波。驻波是指在沿流动方向上某一位置处停滞不动的波, 波速等于零, 特征量随空间变化。目前, 大多数研究主要关注二维行波的时空稳定性分析, 而对于驻波的研究很少, 仅 Alekseenko 和 Brauner 分别在中等雷诺数和高雷诺数范围下研究了等温液膜二维表面驻波的稳定性特征[3~4]。当薄液膜处于蒸发或冷凝条件下, 受界面热非平衡效应的影响, 其边界条件与等温液膜显著不同, 表现为在蒸发或冷凝状态下不仅伴随着相变过程, 而且因波动表面温度分布不均将产生热毛细力效应, 势必将对驻波的稳定性产生一定的影响。本文基于边界层理论和界面热非平衡效应, 采用线性理论方法推导出在蒸发、等温和冷凝状态下普遍适用的线性二维液膜表面驻波空间稳定性方程, 全面分析不同因素对二维表面驻波稳定性的影响规律。

2　驻波空间稳定性方程

温度为 T 的波动薄膜沿倾角为 θ, 温度为 T_w 的固体壁面向下流动, 界面外是温度为 T_s 的饱和蒸汽。假定壁面与液膜间的热量交换完全用于汽液界面间的相变换热; 蒸汽相对汽液界面静止; 冷凝时, 不计非冷凝气体的影响。对于粘性不可压缩流体, 波动降膜的控制方程为边界层方程, 以流函数 Ψ 表示为:

$$\frac{\partial^2\Psi}{\partial t\,\partial y}+\frac{\partial\Psi}{\partial y}\frac{\partial^2\Psi}{\partial x\,\partial y}-\frac{\partial\Psi}{\partial x}\frac{\partial^2\Psi}{\partial y^2}=-\frac{1}{\rho}\frac{\partial p}{\partial x}+g\sin\theta+\nu\frac{\partial^3\Psi}{\partial y^3} \tag{1}$$

边界条件为:

(1) 在固体壁面上, 为无滑移和无渗透条件:

$$y=0,\ \boldsymbol{u}=0 \tag{2}$$

(2) 在汽液界面上, 因蒸发或冷凝作用引起液膜的质量跃变平衡方程为:

$$y=h,\ J=\rho(\boldsymbol{u}-\boldsymbol{u}_i)\cdot\boldsymbol{n}=\rho_v(\boldsymbol{u}_v-\boldsymbol{u}_i)\cdot\boldsymbol{n} \tag{3}$$

(3) 在汽液界面上, 法向应力和切向应力平衡条件为:

$$y=h,\ J=\rho(\boldsymbol{u}-\boldsymbol{u}_v)\cdot\boldsymbol{n}-(\boldsymbol{T}-\boldsymbol{T}_v)\cdot\boldsymbol{n}\cdot\boldsymbol{n}=2K\sigma \tag{4}$$

$$y=h,\ J=\rho(\boldsymbol{u}-\boldsymbol{u}_v)\cdot\boldsymbol{t}-(\boldsymbol{T}-\boldsymbol{T}_v)\cdot\boldsymbol{n}\cdot\boldsymbol{t}=-\Delta\sigma\cdot\boldsymbol{t} \tag{5}$$

式中: t－时间; h－当地液膜厚度; x, y－与流动方向平行和垂直的坐标; g－重力加速度; p, ν－液体的压力和运动粘度; ρ, ρ_v 为液体和蒸汽密度; σ－表

收稿日期: 2003－10－23;　修订日期: 2003－12－10
基金项目: 教育部高等学校博士学科点专项科研基金资助项目(19990079002); 华北电力大学博士学位教师科研基金资助项目(093100014)
作者简介: 叶学民(1973－), 男, 河北邢台人, 华北电力大学讲师.

面张力; J — 质量跃变流率; K — 界面平均曲率; $\boldsymbol{u}$ 和 $\boldsymbol{u}_v$ — 液体和蒸汽的速度; $\boldsymbol{u}_i$ — 液体在界面上的速度; $\boldsymbol{T}$, $\boldsymbol{T}_v$ 分别液体和蒸汽的应力张量; $\boldsymbol{n}$, t 分别为界面处的单位法向矢量和切向矢量。

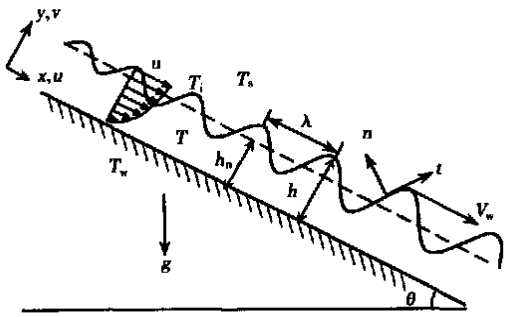

图 1 流动示意图

方程式(3) ~ 式(5) 为因蒸发或冷凝作用引起的界面热不平衡效应, 包括蒸发或冷凝状态以及由此引起的热毛细力对液膜稳定性的影响。Alekseenko 和 Brauner 研究对象为等温液膜[3~4], 因而不包括该方程组。式(4) 假定壁面与液膜间的热量交换完全用于汽液界面间的相变换热:

$$q=\frac{k(T_w-T_i)}{h}=\frac{2a}{2-a}\frac{\rho_v r^2}{T_s}\left(\frac{M}{2\pi R_g T_s}\right)^{1/2}\times(T_i-T_s) \tag{6}$$

因蒸发或冷凝引起的蒸汽压力变化为:

$$p_v=\pm\rho_v\left(\frac{q}{r\rho_v}\right)^2=(-1)^n\frac{1}{\rho_v}\left[\frac{bk\Delta T}{r(1+bh)}\right]^2 \tag{7}$$

式中: $b=\frac{2a}{2-a}\frac{\rho_v r^2}{kT_s}\left(\frac{M}{2\pi R_g T_s}\right)^{1/2}$, $\Delta T=T_w-T_s$ 为壁面过热度; k — 导热系数; T_i — 界面上的液体温度; a — 供应系数; r — 汽化潜热; M — 分子量; R_g — 通用气体常数。当 $n=0$ 时, 表示液膜处于蒸发状态; 当 $n=1$ 时, 液膜处于冷凝状态; 当 $\Delta T=0$ 时, 液膜处于等温状态。

设流函数 $\Psi(x,y,t)=a_0+a_1y+a_2y^2+a_3y^3+a_4y^4$, 其中, $a_i=a_i(x,t)$。假定表面张力随温度的变化为线性关系, 以及在汽液界面处为无滑移条件, 且蒸汽的密度和动力粘度同液体相比可忽略不计, 则 a_i 可由边界条件及边界上的一致性条件求得。采用配置法以汽液界面上的特征量(液膜厚度 h 和表面速度 s) 重新推导控制方程及其边界条件, 经线性化无量纲化处理(推导过程参见文献[9]), 可得:

$$\left(\frac{\partial}{\partial\tilde{\tau}}+2\frac{\partial}{\partial\tilde{X}}\right)H+\frac{Re}{8}\left(\frac{\partial}{\partial\tilde{\tau}}+\frac{\partial}{\partial\tilde{X}}\right)\left(\frac{\partial}{\partial\tilde{\tau}}+\frac{3}{4}\frac{\partial}{\partial\tilde{X}}\right)H+\left(\frac{4B_1+3B_2}{3}\right)\frac{\partial^2H}{\partial\tilde{X}^2}+\frac{Re(B_1-3B_2)}{96}\left(\frac{\partial}{\partial\tilde{\tau}}+\frac{\partial}{\partial\tilde{X}}\right)\times\frac{\partial^2H}{\partial\tilde{X}^2}+\frac{WeRe}{18}\frac{\partial^4H}{\partial\tilde{X}^4}+\frac{WeRe^2}{2304}\left(\frac{\partial}{\partial\tilde{\tau}}+\frac{\partial}{\partial\tilde{X}}\right)\frac{\partial^4H}{\partial\tilde{X}^4}=0 \tag{8}$$

式中: $B_1=(-1)^n\frac{b}{\rho\rho_v g\sin\theta(1+bh_N)^3}\left(\frac{bk\Delta T}{r}\right)^2$, $B_2=\frac{b\gamma\Delta T}{\rho g h_N\sin\theta}\frac{1}{(1+bh_N)^2}$。$B_1$ 表示因蒸发或冷凝引起的汽液界面处蒸汽压力的波动对稳定性的影响, B_2 表示因蒸发或冷凝所引起的热毛细力变化(Marangoni 效应) 对稳定性的影响。S 和 H 是无量纲表面速度和液膜厚度, 为因扰动影响而偏离 Nusselt 解的小量, $S\ll1$, $H\ll1$。h_N 是 Nusselt 平均液膜厚度; γ — 温度系数; $\tilde{X}$ 和 $\tilde{\tau}$ 为沿流动方向的无量纲长度和无量纲时间; We 和 Re 为韦伯数和雷诺数。

方程式(8) 即为二维液膜表面行波线性空间稳定性方程。驻波作为表面行波在空间演化中的一种特殊情形, 波速为零, 其各特征量随空间发生变化。令方程式(8) 中的 $\partial/\partial\tilde{\tau}=0$, 可得:

$$2\frac{\partial H}{\partial\tilde{X}}+\frac{3Re}{32}\frac{\partial^2H}{\partial\tilde{X}^2}+\left(\frac{4B_1+3B_2}{3}\right)\frac{\partial^2H}{\partial\tilde{X}^2}+\frac{Re(B_1-3B_2)}{96}\frac{\partial^3H}{\partial\tilde{X}^3}+\frac{WeRe}{18}\frac{\partial^4H}{\partial\tilde{X}^4}+\frac{WeRe^2}{2304}\left(\frac{\partial^5H}{\partial\tilde{X}^5}\right)=0 \tag{9}$$

方程式(9) 为沿斜壁面下降的在蒸发、等温和冷凝下普遍适用的液膜二维表面驻波线性空间稳定性方程。当 B_1, B_2 等于零时, 就可得到沿倾斜壁面下降的等温液膜二维表面驻波稳定性方程:

$$2\frac{\partial H}{\partial\tilde{X}}+\frac{3Re}{32}\frac{\partial^2H}{\partial\tilde{X}^2}+\frac{WeRe}{18}\frac{\partial^4H}{\partial\tilde{X}^4}+\frac{WeRe^2}{2304}\frac{\partial^5H}{\partial\tilde{X}^5}=0 \tag{10}$$

为分析驻波的空间稳定性特征, 假定扰动在某一空间位置产生, 它仅随空间发生变化, 设此扰动为:

$$H=\tilde{A}\,e^{i\alpha\tilde{X}} \tag{11}$$

式中: $\tilde{A}$ — 扰动幅度。将式(11) 代入式(9) 中, 可得驻波的解方程:

$$\left(i\frac{WeRe^2}{4608}\right)\alpha^4+\frac{WeRe}{36}\alpha^3+\left[i\frac{Re}{192}(3B_2-B_1)\right]\times\alpha^2+\left(-\frac{3Re}{64}-\frac{2B_1}{3}-\frac{B_2}{2}\right)\alpha+i=0 \tag{12}$$

在空间稳定性分析中, α 为复数, $\alpha=\alpha_r+i\alpha_i$。$\alpha_r$ 表示波数, $-\alpha_i$ 表示扰动空间增长率。$-\alpha_i>0$ 表

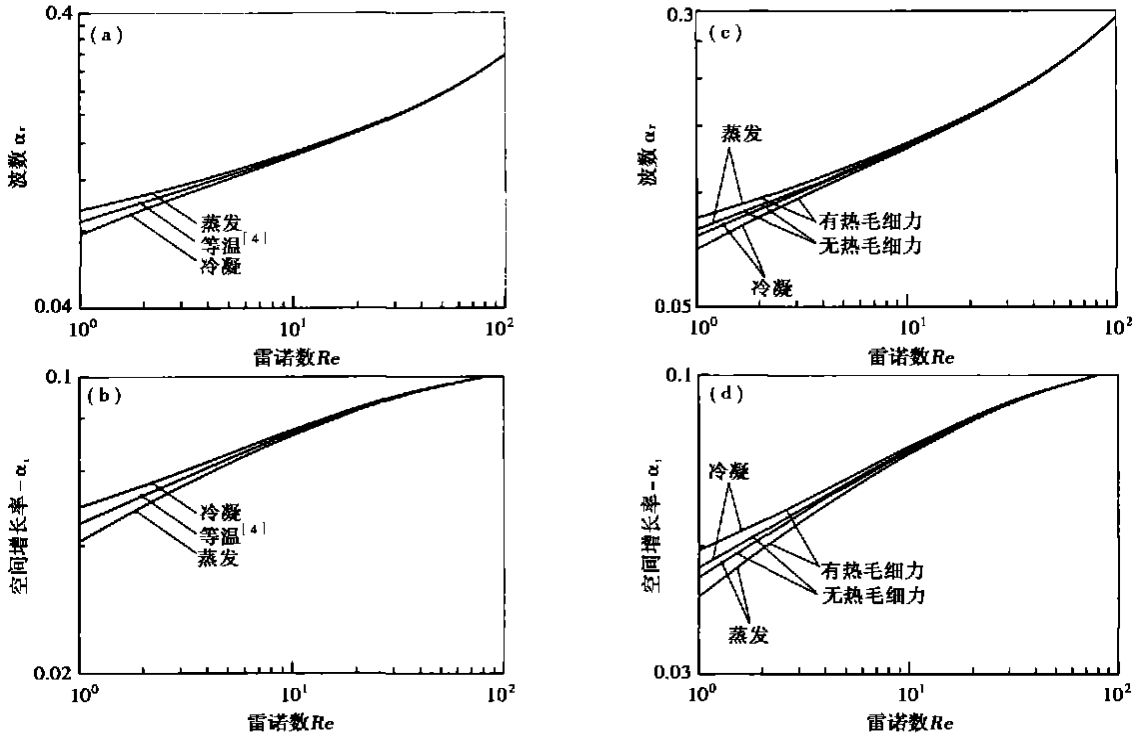

图 2　驻波的空间稳定性曲线。(a) ~ (b) 蒸发、等温或冷凝状态的影响;
(c) ~ (d) 蒸发或冷凝状态下热毛细力的影响

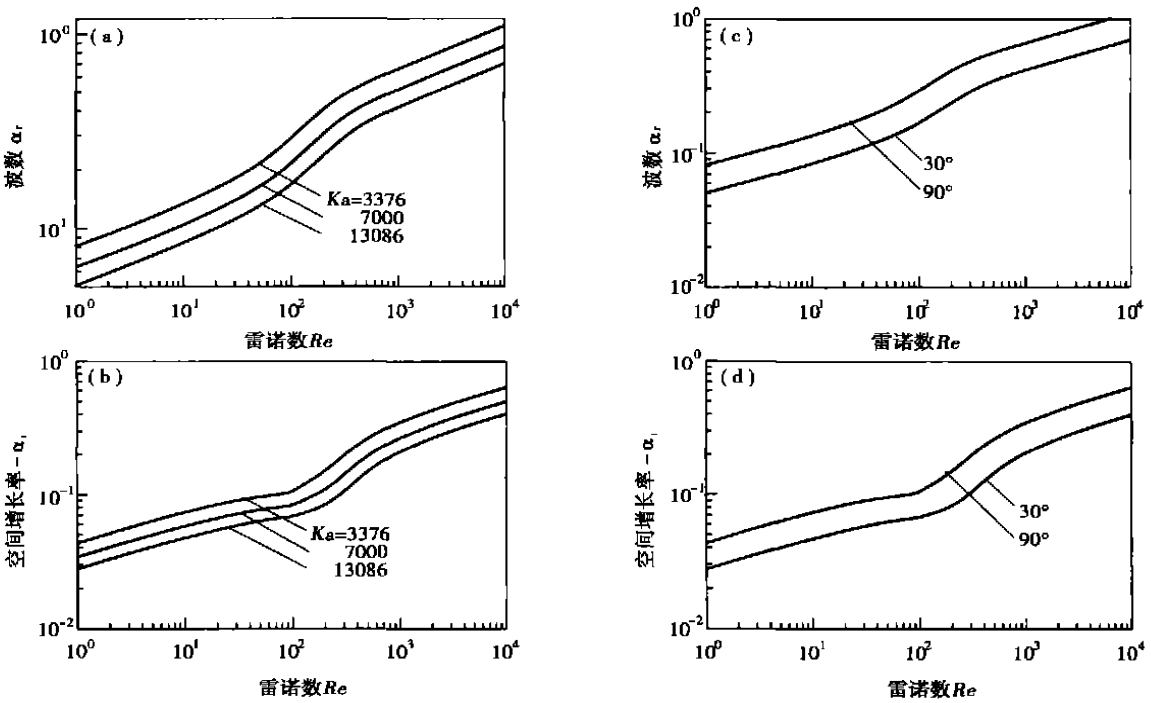

图 3　驻波的空间稳定性曲线。(a) ~ (b) 物性 Ka 的影响;(c) ~ (d) 倾角的影响

示扰动随空间是增长的, 稳定性减弱; $-\alpha_i < 0$ 表示扰动随空间是衰减的, 稳定性增强; $-\alpha_i = 0$ 时为中性稳定。

由方程式(9)和式(12)可知, α 也可表示为:

$$\alpha = f(Re, Ka, \theta, B_1, B_2) \tag{13}$$

其中: $Ka = \frac{\sigma}{\rho g^{1/3} \nu^{4/3}}$, 为Kapitza 数。$Ka$ 和θ 隐含在方程中, 分别代表流体物性和倾斜角度的影响。Re 代表惯性力和粘性力的影响, B_1 和 B_2 分别代表因蒸发或冷凝引起汽液界面处蒸汽压力的波动和热毛细力变化的影响。

3 计算结果分析

对于方程式(12), 只有当 $\alpha_r > 0$, $\alpha_i < 0$ 的解才是有物理意义的解。通过数值计算, 在图 2 和图 3 中给出了工质为水的驻波的波数和空间增长率在不同条件下随雷诺数的变化曲线。

图2 和图 3 显示, 驻波的波数和空间增长率随雷诺数的增大呈现单调增加趋势, 表明驻波空间稳定性逐渐丧失。图 2(a)和 2(b)表明, 与液膜处于等温状态相比[4], 液膜处于蒸发状态下的驻波波数有所增加, 空间增长率减弱, 而冷凝状态下的波数有所减小, 空间增长率增强。图 2(c)和 2(d)表明, 在蒸发状态下, 热毛细力促进波数有所增大, 并减弱空间增长率, 在冷凝状态下, 热毛细力促使波数有所减小, 并增强空间增长率。这是因为对处于蒸发或冷凝状态下的液膜, 受界面热非平衡效应的影响, 将引起蒸汽压力作用(蒸汽反作用力), 而且因波动表面的温度分布不均将产生热毛细力效应, 导致汽液界面条件与等温情形明显不同, 并将影响液膜空间的流动稳定性。另外, 由图 2 可知, 在不同雷诺数下, 蒸发或冷凝以及毛细力的作用对驻波波数和空间增长率的影响程度也不尽相同。在小雷诺数下($Re < 50$), 蒸发或冷凝以及毛细力的作用比较明显, 因此, 液膜空间稳定性受其影响较为显著。随着雷诺数的增大($Re > 50$), 该作用逐渐减小, 此时, 惯性力和粘性力的作用占主导地位, 空间稳定性几乎不受蒸发或冷凝以及热毛细力的影响。

图 3(a)和 3(b)表明, 驻波的波数和空间增长率随 Ka 数的增加而减小, 在这里, 以 Ka 数表示物性的影响, Ka 数越大, 说明液体温度越高。图 3(c)和 3(d)表明, 波数和空间增长率随倾角的增加而变大, 当薄液膜沿垂直固体壁面流动时, 其空间增长率最大, 此时, 流动处于最不稳定状态, 这同 Benjamin 和 Yih 的研究结果一致[1~2]。图 3 还表明, 与蒸发或冷凝状态和热毛细力的作用不同, 物性 Ka 数和倾角对驻波的波数和空间增长率的影响在整个雷诺数范围内均比较明显。

4 结 论

基于边界层理论和界面热非平衡效应条件, 采用配置法, 推导出了沿倾斜壁面下降的在蒸发、等温和冷凝状态下普遍适用的液膜二维表面驻波线性空间稳定性方程, 包含了蒸发、等温和冷凝等不同状态、热毛细力、雷诺数、流体物性和壁面倾角对驻波空间稳定性的影响。

研究表明: 蒸发有利于驻波空间稳定性, 冷凝不利于稳定; 在蒸发状态下, 热毛细力促进其稳定, 在冷凝状态下, 则导致其失稳; 稳定性随倾角和雷诺数的增大而减小, 随 Ka 数的增大而加强。在小雷诺数下, 蒸发或冷凝以及热毛细力作用对驻波稳定性的影响仅在 $Re < 50$ 范围内比较明显。随着雷诺数的增加, 稳定性主要取决于惯性力和粘性力的相对大小; 流体物性和壁面倾角在整个雷诺数范围内对其稳定性起着非常明显的作用。

参考文献:

[1] BENJAMIN G B. Wave formation in laminar flow down an inclined plane[J]. **J Fluid Mech**, 1957, **2**: 554—574.

[2] YIH C S. Stability of liquid flow down an inclined plane[J]. **Phys Fluids**, 1963, **6**(3): 321—335.

[3] ALEKSEENKO S V, NAKORYAKOV V E, POKUSAEV B G. Wave formation on vertical falling liquid films[J]. **Int J Multiphase Flow**, 1985, **11**(5): 607—627.

[4] BRAUNER N, MARON D M, ZIJL W. Interfacial collocation equations of thin liquid film: stability analysis[J]. **Chem Engng Sci**, 1987, **42**(8): 2025—2035.

[5] JOO S W, DAVIS S H, BANKOFF S G. Long-wave instabilities of heated films: two-dimensional theory of uniform layers[J]. **J Fluid Mech**, 1991, **230**: 117—146.

[6] BOHN M S, DAVIS S H. Thermocapillary breakdown of falling liquid films at high reynolds numbers[J]. **Int J Heat Mass Transfer**, 1993, **36**(7): 1875—1881.

[7] YU L, WASDEN F, DUKLER A E, et al. Non-linear evolution of waves on falling films at high Reynolds numbers[J]. **Phys Fluids**, 1995, **7**(8): 1886—1902.

[8] 叶学民, 阎维平. 沿倾斜壁面下降的蒸发或冷凝降膜二维表面波的线性稳定性[J], 西安交通大学学报, 2002, **36**(1): 25—30.

[9] 叶学民, 阎维平. 蒸发或冷凝薄液膜的空间稳定性分析[J], 中国电机工程学报, 2002, **22**(12): 26—31.

coal-based chemical industries, energy comprehensive utilization systems and near-zero pollutant emission systems. Pressurized oxygen-blown gasification fed with dry pulverized coal represents a main direction of development for coal gasification technology. The authors briefly describe a test system of pressurized coal gasification fed with dry pulverized coal, which has been set up in a Thermal Engineering Research Institute. The study and test results of the above system are given. With the clarification of the law of pressurized coal gasification fed with dry pulverized coal the tests have attained the anticipated aim. In addition, the operational stability of the test system under high pressures have also been verified. **Key words**: coal gasification, entrained flow, dry feed of pulverized coal

超细煤粉还原 NO_x 的试验研究＝**Experimental Investigation of Super Fine Pulverized-coal Reburning Technology for Reducing NO_x emissions** [刊, 汉] / JIN Jing, LI Rui-yang, ZHANG Zhong-xiao (College of Power Engineering under the Shanghai University of Science &Technology, Shanghai, China, Post Code: 200093) // Journal of Engineering for Thermal Energy &Power. — 2004, 19(6). —582～585.

Ultra-fine pulverized coal reburning technology features high-efficiency NO_x reduction, low operating costs and ease of implementation. Through tests the authors have studied the key factors in this reburning technology, which exercise a major influence on NO_x reduction. The results of this study indicate that the finer the reburned fuel particles, the higher the NO_x reduction efficiency. The optimum average particle diameter of the reburned fuel is 20 μm. The optimum ratio of reburned fuel is 20% for lignite of Longkou and 25% for bituminous coal of Shenfu. There exists an optimum injection location for the reburned fuel. In general, the higher the coal rank, the further is the distance from a main fuel nozzle. The residence time of fuel in the optimum reburning zone is 0.63 s for lignite of Longkou and 0.75 s for bituminous coal of Shenfu. **Key words**: super fine pulverized coal, reburning, NO_x, reduction efficiency

一种基于差压波动图的段塞流识别方法＝**Slug-flow Identification Method Based on a Differential-pressure Fluctuation Diagram** [刊, 汉] / LIANG Fa-chun, WANG Dong, LIN Zong-hu (National Key Laboratory on Multi-phase Flows in Power Engineering under the Xi' an Jiaotong University, Xi' an, China, Post Code: 710049) // Journal of Engineering for Thermal Energy &Power. — 2004, 19(6). —586～588.

Extensive air-water two-phase flow tests were conducted on a large-sized horizontal test loop of multi-phase flows made of steel pipe of 80 mm inner diameter. The differential-pressure fluctuation signals of stratified, slug and annular flow patterns collected in a certain length of time were displayed as two-dimensional images. Through an analysis of 30 groups of differential-pressure fluctuation data it has been found that the ratio between signal zone area and background zone area has an average value of 0.026 for the slug flow, 0.53 for the stratified flow and 0.35 for the annular flow. The ratio between slug-flow signal zone and the total image area is considerably smaller than that of the other flow patterns. Consequently, this ratio can be taken as a characteristic parameter for slug-flow identification. The method under discussion can be effectively employed for the rapid and automatic detection of slug flow patterns. **Key words**: slug flow, flow pattern identification, differential-pressure fluctuation, image

薄液膜二维表面驻波的流动稳定性研究＝**Flow Stability Investigation of Two-dimensional Surface Stationary Waves on a Thin Liquid Film** [刊, 汉] / YE Xue-min, LI Chun-xi, YAN Wei-ping (Department of Power Engineering, North China Electric Power University, Baoding, China, Post Code: 071003) // Journal of Engineering for Thermal Energy &Power. — 2004, 19(6). —589～592.

The flow stability of stationary waves, a kind of surface wave on a thin-liquid film, is subject to the influence of thermal non-equilibrium effect at a vapor-liquid interface. On the basis of boundary layer theory and thermal non-equilibrium effect derived is a spatial stability equation of the two-dimensional surface stationary waves universally applicable on evaporating, isothermal or condensing liquid films draining down along an inclined wall. From a theoretical viewpoint an in-

depth analysis was conducted of the influence of thermal non-equilibrium effect, fluid physical properties, wall surface inclination angle and Reynolds number on the stability of stationary waves. The results of the study indicate that the influence of thermal non-equilibrium effect on the stability of the stationary waves is relatively significant only under small Reynolds numbers. At higher Reynolds numbers the stability is mainly dependent on inertial force and viscosity force. In the whole range of Reynolds number, fluid physical properties and wall surface inclination angle all play a very conspicuous role. **Key words**: evaporation, cooling, thermal non-equilibrium effect, thin liquid film, stationary wave, stability

汽液相变换热过程唯象系数的计算＝**Calculation of Phenomenological Coefficient in the Heat Exchange Process of Liquid-vapor Phase Transition** [刊, 汉] / WU Shuang-ying, ZENG Dan-ling (College of Power Engineering under the Chongqing University, Chongqing, China, Post Code: 400044) // Journal of Engineering for Thermal Energy & Power. — 2004, 19(6). —593 ~596.

In the light of the theory of non-equilibrium thermodynamics derived is formula for calculating the chemical potential variation and vapor bubble critical radius in the heat exchange process of liquid-vapor phase transition. On this basis, a phenomenological coefficient is proposed to evaluate the intensity of phase-transition heat exchange process. Meanwhile, a formula for calculating the phenomenological coefficient of phase-transition heat exchange process is given and a numerical calculation performed. The impact of the driving force of the phase-transition process, and bubble radius, etc on the phenomenological coefficient is also discussed. **Key words**: phase transition, phenomenological coefficient, non-equilibrium thermodynamics

有叶扩压器内部流场的 PIV 实验测量＝**PIV（Particle Image Velocimetry）Experimental Measurements of the Flow Field in a Bladed Diffuser** [刊, 汉] / ZHANG Li, WANG Qi-jie (Power Engineering Department, Shanghai Electric Power Institute, Shanghai, China, Post Code: 200090), CHEN Han-ping (Mechanical College under the Shanghai Jiaotong University, Shanghai, China, Post Code: 200030) // Journal of Engineering for Thermal Energy & Power. — 2004, 19(6). —597 ~600.

By making use of PIV (particle image velocimetry) techniques capable of acquiring an instantaneous velocity field an experimental investigation is conducted of the flow in a bladed diffuser. The flow field in the diffuser at different flow conditions was measured. The test data were processed by the use of an integral averaged method and diagrams showing velocity field distribution at various flow conditions were obtained. An analysis and discussion of the above was also conducted. **Key words**: bladed diffuser, experimental measurement, particle image velocimetry

CFD 技术在汽轮机定子线圈冷却水流量测量中的应用＝**The Application of CFD（Computational Fluid Dynamics）Technology for the Measurement of Cooling Water Flow in a Turbogenerator Stator Coil** [刊, 汉] / XIAO Hui-min, YANG Jian-dong (National Key Laboratory of Water Resources & Hydropower Engineering Sciences under the Wuhan University, Wuhan, China, Post Code: 430072) // Journal of Engineering for Thermal Energy & Power. — 2004, 19(6). —601 ~604.

By using an ultrasonic flowmeter to detect and measure the flow rate of cooling water in a large-sized turbogenerator stator coil it is possible to directly ascertain whether there exists a phenomenon of cooling water jamming and leak, thus thoroughly solving the problem of cooling water blocking. However, when the ultrasonic flowmeter is used for conducting measurements in a curved tube section, errors may occur. By using CFD (computational fluid dynamics) technology the authors have calculated the cooling-water flow velocity distribution in the generator stator coil at a thermal power plant and analyzed the influence of in-tube flow on ultrasonic flow gauging. As a result, the variation tendency of measurement errors at various measuring locations was obtained. The use of CFD technology makes it possible to determine the optimum installation location for an ultrasonic flowmeter, thus providing a theoretical basis for obtaining an accurate flow rate. **Key words**: ultrasonic flowmeter, curved pipe, computational fluid dynamics